Investigation of the Pore Structure and Morphology of Cellulose Acetate Membranes Using Small-Angle Neutron Scattering. 2. Ultrafiltration and Reverse-Osmosis Membranes

Sandeep Kulkarni† and Sonja Krause*

Polymer Science and Engineering Program & Department of Chemistry, Rensselaer Polytechnic Institute, Troy, New York 12180

G. D. Wignall

Solid State Division, Oak Ridge National Laboratory, Oak Ridge, Tennessee 37831

Received February 22, 1994®

ABSTRACT: Pore structure in cellulose acetate ultrafiltration (UF) and reverse-osmosis (RO) membranes has been studied using small-angle neutron scattering. Scattering experiments were carried out on dry membranes as well as on membranes swollen with deuterated solvents (D_2O and CD_3OD). In addition, the RO membranes were studied both before and after annealing (a process of heating a membrane in a water bath at ~75 °C to improve its separation properties). The pore surface in UF membranes was found to be smooth and nonfractal, as evidenced by the fourth power law behavior at high **Q**. Values of average pore sizes obtained for dry and solvent swollen membranes agree well with pore sizes obtained by other methods. For cellulose acetate RO membranes in their dry state, the unannealed membrane appears to consist of two discrete pore size distributions in the intermediate and high **Q** region while the annealed membrane contains a much wider distribution of pore sizes. These results give a good account of the changes occurring in the structure of RO membranes as a result of annealing, and agree well with the predictions of other authors.

Introduction

A large number of synthetic polymeric membranes, in current commercial use, can be classified as either reverse-osmosis (RO) or ultrafiltration (UF) membranes. While these two types of membranes differ in their separation properties or selectivity toward various solutes (RO membranes are much more selective than UF membranes), they have numerous intrinsic similarities. For instance, as was previously mentioned,[1] RO and UF membranes in general have an asymmetric structure; i.e., they both consist of a thin and relatively dense skin layer overlaid on a thick and highly porous base layer.

The morphology of RO and UF membranes has been delineated in some detail by Kesting[2] recently (his description is based on the information provided by electron microscopy on such membranes). Kesting has essentially proposed the simultaneous existence of the following four levels of structure in a membrane: macromolecules (individual chain), nodules (aggregates of polymer chains), nodular aggregates, and supernodular aggregates. On the basis of this picture he suggested that the skin layer in RO membranes consists of mainly nodules with a few nodular aggregates present. The structure is rather compact and the functional pores are primarily the interstitial voids between closely packed nodules. In the case of UF membranes, Kesting suggests that the skin layer is primarily composed of nodular aggregates and the pores in this case are the spaces or voids between individual nodular aggregates. Thus there appears to be structural similarity between RO and UF membranes which in turn indicates similarities in the mechanism of their formation.

In our preceding publication[1] the structure of the "skin layer" (surface) in asymmetric RO membranes was discussed, using the active layer membranes as the model system. Due to the proposed structural similarity between RO and UF membranes, it appeared logical to study the skin layer in UF membranes using similar means. However, no published methods for the preparation of active layers of UF membranes (analogous to the active layers in RO membranes) could be found in the membrane literature. For this reason, this paper involves a study of only *complete* UF membranes (skin layer plus the porous base layer), prepared from cellulose acetate, in an attempt to understand the surface pore structure. For effective comparison, samples of *complete* (asymmetric) RO membranes were also studied. It must be realized that in both cases the contribution due to the base layer to the overall scattering is expected to make the analysis somewhat more difficult.

As described previously,[1] small-angle neutron scattering experiments were performed both on dry and swollen (with D_2O and/or CD_3OD) membranes.

Experimental Section

General. Details of the polymer and solvents used in this work are given in the previous publication.[1]

Membrane Preparation. Cellulose acetate RO membranes were prepared by the procedure of Manjikian.[3] A casting solution consisting of cellulose acetate, formamide, and acetone (in the weight ratio 21.4/14.2/64.4) was cast on a glass plate at −10 ± 1 °C. After an evaporation period of ~10 min, at the same temperature, the plate was immersed in an ice bath for 1 h to cause gelation of the polymer film. The membrane so formed will be referred to as "unannealed membrane" in later discussions. Portions of this membrane were then "annealed" by immersing them in a water bath at 73 ± 1 °C for 5 min (this process improves the separation properties of the membrane). This membrane will be subsequently referred to as "annealed membrane". Both unannealed and annealed membranes were kept soaked in water because the pore structure collapses if the membrane is allowed to dry in air.[4]

Cellulose acetate UF membranes were prepared[5] by casting a mixture of cellulose acetate, acetone, and formamide in the weight ratio 17/30/53, on a glass plate at room temperature. After a very short evaporation period (~5 s) in air, the plate was immersed in an ice bath for 1 h for gelation to take place. These membranes were also stored wet to preserve their pore structure.

A solvent exchange process originally described by Lui[6] was used to prepare dry RO and UF membranes. In this procedure

† Present address: Department of Polymer Science and Engineering, University of Massachusetts, Amherst, MA 01003.

® Abstract published in *Advance ACS Abstracts*, October 1, 1994.

0024-9297/94/2227-6785$04.50/0 © 1994 American Chemical Society

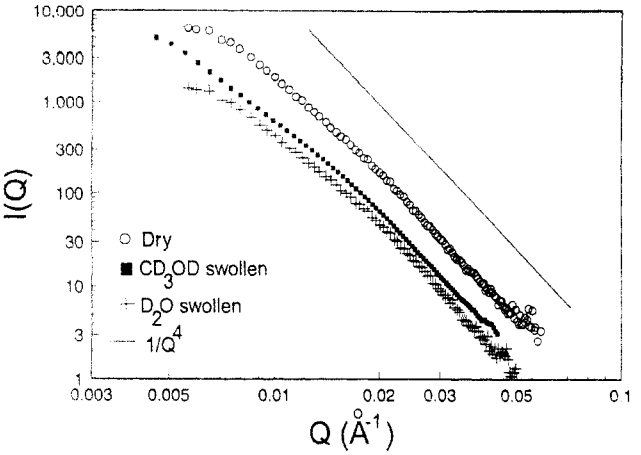

Figure 1. Scattering curves for dry, D_2O swollen, and CD_3OD swollen UF membranes.

the wet membranes were immersed in a 25 vol % solution of ethanol in water and allowed to stand overnight. The process was repeated using 50, 75, and 100% ethanol–water mixtures successively. Following this, the membrane was immersed in hexane for ~12 h. The membrane was then removed and air-dried to evaporate all the hexane. The resultant dry membranes were usually turbid in appearance.

Small-Angle Neutron Scattering. Small-angle neutron scattering (SANS) experiments were performed either at Oak Ridge National Laboratory (ORNL) or at the National Institute of Standards and Technology (NIST) and the details of the instruments, the sample cell used, and the data collection process have been described earlier.[1]

The equations used for analysis of the scattering data were also discussed in the previous paper. The basic expression involved is the Debye–Bueche equation,[7] for a random two-phase system, of the form:

$$\frac{d\sum(\mathbf{Q})}{d\Omega} = (\rho_1 - \rho_2)^2\phi(1-\phi)4\pi\left[\frac{2fa_1^3}{(1+\mathbf{Q}^2a_1^2)^2} + \frac{(1-f)\pi^{1/2}a_2^3}{4}\exp\left(-\frac{\mathbf{Q}^2a_2^2}{4}\right)\right] \quad (1)$$

where ρ_1 and ρ_2 are the scattering length densities of the two phases, ϕ is the volume fraction of one phase, a_1 and a_2 are the short-range correlation length and long-range correlation length, respectively, and f is the fractional contribution of one of the terms. Furthermore it was also determined in that study that for membranes composed of structures (where "structures" may refer either to pores or to the polymer aggregates forming the membrane) of a range of different sizes, the single exponential term in eq 1 must be replaced by a *sum of exponentials* (see eq 6 in ref 1). Each of these exponential terms contains a particular value of the long-range correlation length, reflecting the average size of a particular type of structure present in the membrane. The values of the long-range correlation lengths can be obtained by fitting the low **Q** region of the scattering curve to a multiexponential expression, using a FORTRAN program called DISCRETE.[8,9]

Results and Discussion

The scattering curves for a dry, a D_2O swollen, and a CD_3OD swollen UF membrane are shown plotted on a log–log scale in Figure 1. The straight line in this figure has a slope of −4 and is drawn to check whether the experimental scattering curves follow the Porod's fourth power law at high **Q**. All three curves in Figure 1 exhibit the Porod law dependence over a rather large **Q** range. Using the concepts developed by Bale[10] and Schmidt[11] for scattering from the porous system with fractal surfaces (as discussed in some detail in our previous paper), the Porod law behavior implies that the pores in UF membranes are smooth, well-defined, and essentially nonfractal (fractal dimension = 2.0) within the limits of resolution of the scattering experiment.

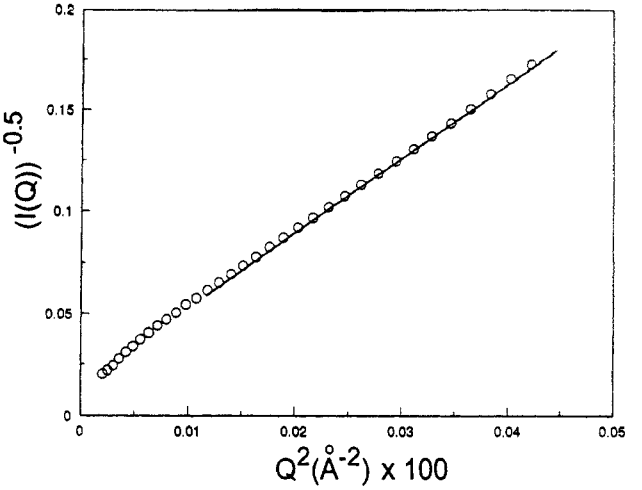

Figure 2. $(I(\mathbf{Q}))^{-0.5}$ vs $\mathbf{Q}^2$ plot for a dry UF membrane.

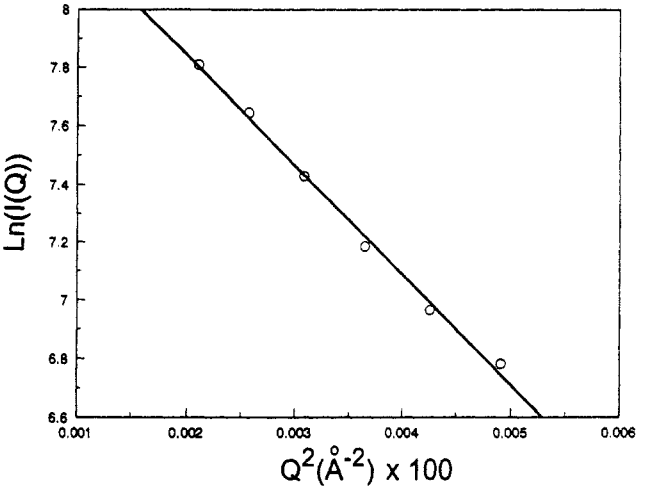

Figure 3. ln $I(\mathbf{Q})$ vs $\mathbf{Q}^2$ plot of the data at very low **Q** for a dry UF membrane.

Next, the data at lower **Q** values were analyzed using the Debye–Bueche model. A plot of $(I(\mathbf{Q}))^{-0.5}$ vs $\mathbf{Q}^2$ for the dry UF membrane is shown in Figure 2. The plot has a large linear region although there is noticeable deviation from linearity at very low **Q**. A fit to the linear region in Figure 2 gave the following value for the short-range correlation length for the dry UF membrane:

$$a_{1,\mathrm{dry}} \cong 140 \text{ Å}$$

The characteristic pore dimension as given by the short-range correlation length is comparable in magnitude to the dimensions of pores (roughly 150–300 Å) observed on the surface of UF membranes by electron microscopy. Figure 3 shows the ln $I(\mathbf{Q})$ vs $\mathbf{Q}^2$ plot of the data at the lowest **Q** values obtained for the dry UF membrane (the first term in eq 1 makes a negligible contribution at the lowest **Q** values; hence, it was not considered necessary to subtract this term from the low **Q** data). Although the number of data points in this region is insufficient for an exact analysis, the data *approximately* fits a linear relationship as shown in Figure 3, giving the following value for the long-range correlation length:

$$a_{2,\mathrm{dry}} \cong 388 \text{ Å}$$

This value is of the same order as the sizes of the nodular

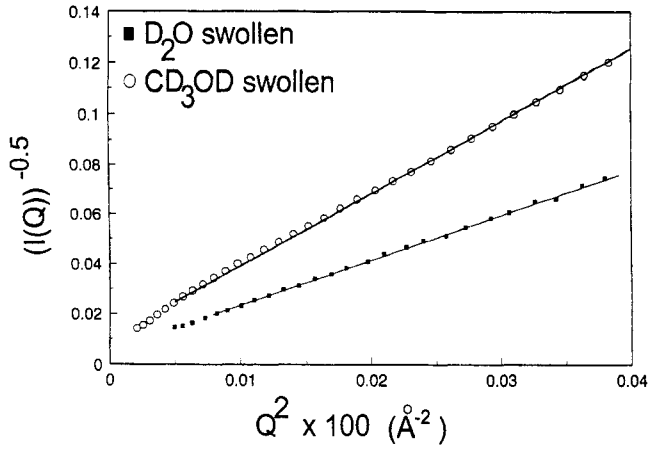

Figure 4. $(I(\mathbf{Q}))^{-0.5}$ vs $\mathbf{Q}^2$ plots for D_2O and CD_3OD swollen UF membranes.

aggregates observed by electron microscopy, and hence it is likely that the long-range correlation length reflects on the type of aggregates present on the surface. However, it is equally likely that this value corresponds to radii of larger pores present below the surface. In the absence of data from the surface (skin) layer *alone*, for the reason mentioned in the Introduction, it is impossible to determine if either one or *both* these contributions are present.

Figure 4 shows $(I(\mathbf{Q}))^{-0.5}$ vs $\mathbf{Q}^2$ plots for UF membranes swollen with D_2O and CD_3OD. Unlike the dry membrane, the curves are linear virtually over the *entire* $\mathbf{Q}$ range (the CD_3OD swollen membrane shows some nonlinearity at extremely low $\mathbf{Q}$, but this region is much smaller than the one observed in the case of the dry membrane). A fit to the two curves gave the following (single) values of correlation lengths:

$$a_{D_2O} = 180 \text{ Å}$$

$$a_{CD_3OD} = 160 \text{ Å}$$

These values are somewhat larger than the short-range correlation length obtained for the dry membrane (140 Å), and this reflects an increase in pore size due to swelling, as expected. It is interesting to note that the CD_3OD swollen membrane shows a smaller change in pore size as compared to the D_2O swollen membrane. A similar result was obtained in our study[1] of D_2O and CD_3OD swollen active layer membranes and, as discussed therein, is most likely related to the different abilities of D_2O and CD_3OD to hydrogen bond with cellulose acetate. D_2O forms stronger hydrogen bonds and hence is able to accommodate a larger thickness of the "hydration sheath" (water present as ordered clusters in a pore) on swelling which can in turn be related to a larger pore radius.

Figure 5 shows the log–log scattering plots for unannealed and annealed RO membranes in their dry state. The curve for the unannealed membrane can be seen to undergo a rather abrupt change in slope at $\log \mathbf{Q} \cong -1.35$ ($\mathbf{Q} \cong 0.045$ Å^{-1}), where a cross-over of the two curves also occurs. The curve for the unannealed membrane exhibits a fourth power law dependence over a limited range of $\mathbf{Q}$ values, i.e., in the region $-1.35 < \log \mathbf{Q} < -1$ (0.045 Å^{-1} < $\mathbf{Q}$ < 0.1 Å^{-1}), as indicated by the arrows in Figure 5. The curve for the annealed membrane, on the other hand, has no power law region. In the high $\mathbf{Q}$ region, the annealed sample has higher scattering than the unannealed membrane while the situation is reversed in the low $\mathbf{Q}$ region.

It is important to consider the implication of a power law behavior in the intermediate $\mathbf{Q}$ region, since such a

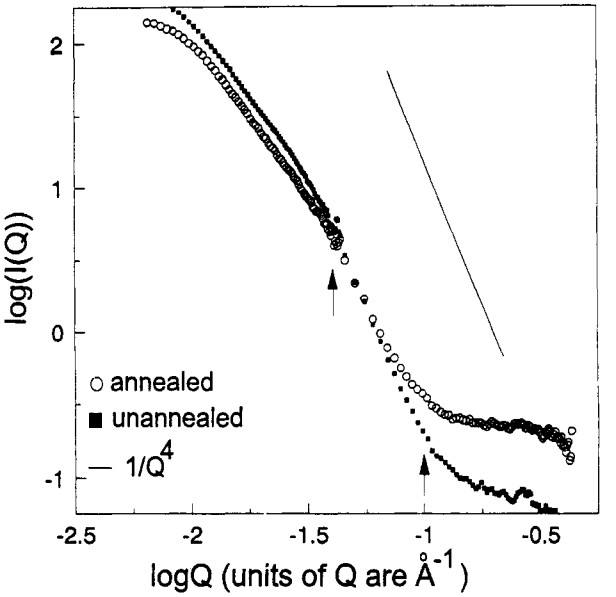

Figure 5. Scattering plots for unannealed and annealed RO membranes in their dry state.

dependence is usually observed only at very high $\mathbf{Q}$ values.[12] Scattering in the Porod's law region originates from *surfaces* of the scattering objects, in contrast to the rest of the scattering curve which reflects *volume or bulk scattering* from the objects. Hence Porod's law is observed *only* when there is no contribution due to *volume scattering* from the objects. Vice versa, the fact that Porod's law is observed in a *certain* $\mathbf{Q}$ *(intermediate) region* of a scattering curve indicates that there are no structures present in the system which would exhibit volume scattering *in that region*. Since a $\mathbf{Q}$ range can be related to a range of sizes "d" ($\mathbf{Q} \cong 2\pi/d$), the above argument in turn implies an absence of structures of a certain *size range* when Porod's law is observed at intermediate $\mathbf{Q}$ values and only over a limited $\mathbf{Q}$ range.

For the unannealed RO membranes, therefore, the power law observed in the intermediate $\mathbf{Q}$ region (0.045 Å^{-1} < $\mathbf{Q}$ < 0.1 Å^{-1}) implies that pores in the size range ~30–60 Å, which would scatter in the above $\mathbf{Q}$ region, are absent. This in turn indicates that the pore size distribution in the unannealed membrane changes quite sharply from the base layer of the membrane to the skin layer. The annealed membrane, however, appears to contain pores of a broad range of sizes, as evidenced by the rather gradual decrease in scattered intensity. Also, comparing the relative magnitudes of scattered intensities at low and high $\mathbf{Q}$, it can be seen that the unannealed membrane contains a higher proportion of large pores as compared to the annealed membrane. On the other hand, the annealed membrane seems to contain a larger proportion of *very small* pores relative to the unannealed membrane.

A plot of $(I(\mathbf{Q}))^{-0.5}$ vs $\mathbf{Q}^2$ for the high $\mathbf{Q}$ region of the dry membranes is shown in Figure 6. The curves in Figure 6 show a large linear portion, and a fit to this region of the plot gave the following values for the short-range correlation length (a_1):

$$a_1(\text{unannealed membrane}) \cong 5 \text{ Å}$$

$$a_1(\text{annealed membrane}) \cong 3 \text{ Å}$$

It is known that the process of annealing improves the separation properties of the membrane by "shrinking" the pores on the surface, i.e., reducing the pore size. The values for the short-range correlation length appear to reflect this trend.

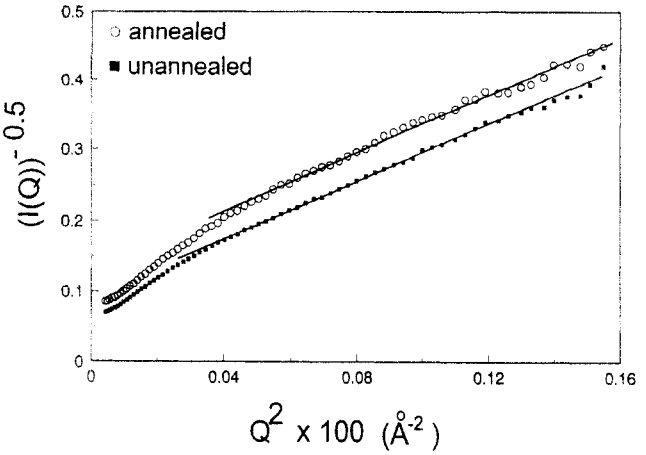

Figure 6. $(I(\mathbf{Q}))^{-0.5}$ vs $\mathbf{Q}^2$ plots for the high $\mathbf{Q}$ region of dry RO membranes.

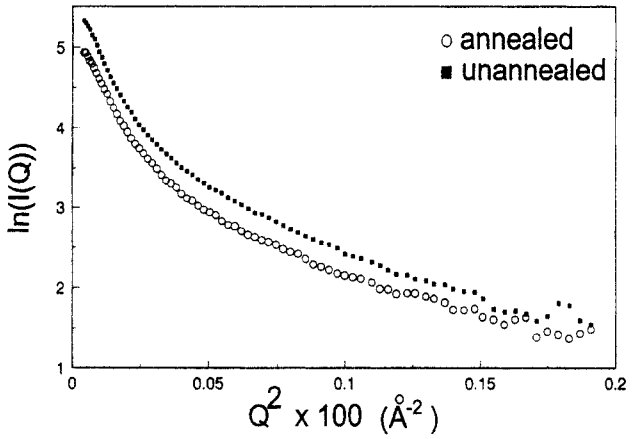

Figure 7. $\ln I_{diff}(\mathbf{Q})$ vs $\mathbf{Q}^2$ plots for the low $\mathbf{Q}$ region of unannealed and annealed RO membranes in their dry state.

Next, the contribution due to the high $\mathbf{Q}$ term was subtracted from the Debye–Bueche expression (eq 1) to obtain $I_{diff}(\mathbf{Q})$, which contains only the exponential term as discussed previously.[1] Figure 7 shows a plot of ln $I_{diff}(\mathbf{Q})$ vs $\mathbf{Q}^2$ for the unannealed and the annealed membranes. It is clear that the relationship is multiexponential in both cases and therefore DISCRETE was used to fit both sets of data. This gave the following values for the long-range correlation length:

unannealed: a_2 = 135 and 60 Å

annealed: a_2 = 130, 60, and 20 Å

In the case of the active layer membranes studied earlier,[1] the values of the long-range correlation length could be unambiguously assigned to spacing between pores (which reflects the sizes of aggregates present) since there were clearly no large (>20 Å) pores present. For the RO membranes, however, the values of the long-range correlation lengths may correspond *either* to different *pore size distributions* or to the different *spacing* between pores or *both*. This is because an RO membrane is known to contain a wide range of pore sizes in the base layer (though not in the skin layer) which would also contribute to the scattering pattern. In fact, it can be assumed that scattering from such pores forms the major component of the long-range correlation lengths since many such pores are present in the base layer. Furthermore, the values of the long-range correlation length obtained above are in the range 20–130 Å, which is too small to correspond to the sizes of structures (nodules or nodular aggregates)

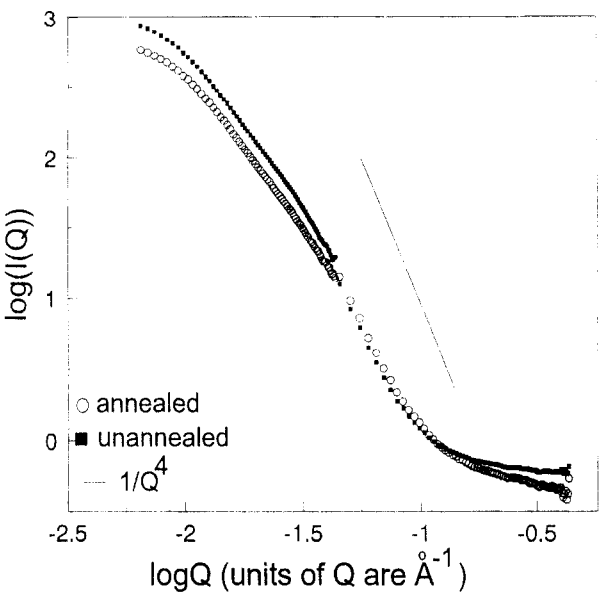

Figure 8. Scattering curves for D_2O swollen unannealed and annealed RO membranes.

present in the membrane. The range of values obtained for the annealed membrane indicate that there may be a more continuous distribution of values of a_2 than the discrete intervals given above. This also confirms the prediction that, as compared to the unannealed membrane, the annealed membrane contains a much wider range of pore sizes. It should be noted that a similar approach was used by Statton[13] many years ago to determine the range of void sizes in cellulose fibers, and his method involved resolving a log–log scattering curve into successive tangents each of which provided a value for the void size.

The log–log scattering curves for D_2O swollen unannealed and annealed membranes are shown in Figure 8. It is clear from these plots that the distinct differences which were observed between the dry unannealed and annealed membranes are almost completely washed out upon introduction of D_2O in the samples. Both curves show similar slopes over the entire range of $\mathbf{Q}$ values. It is particularly interesting to note that the D_2O swollen unannealed membrane shows no abrupt change in slope or a fourth power law behavior in the intermediate $\mathbf{Q}$ region (as observed in the case of the dry membrane). Hence the D_2O swollen membrane appears to contain a wide range of pore sizes and, unlike the dry membrane, there are no "excluded" pore sizes. The difference most likely arises because of an increase in size of the small pores (<30 Å in radius) due to swelling, which consequently exhibit volume scattering at somewhat lower $\mathbf{Q}$ values and hence in the region where only surface scattering (i.e. the Porod's law) was observed prior to swelling.

The modified Debye–Bueche equation used to analyze the dry membranes was also employed for the D_2O swollen membranes to obtain values of short-range and long-range correlation lengths. Due to the almost identical shape of the curves, very similar values were obtained for *both* the unannealed and annealed membranes. Hence only one set of correlation lengths has been quoted below:

short-range correlation length: $a_1 \cong 5$ Å

long-range correlation lengths: $a_2 \cong 25$, 50, and 150 Å

Once again, these values for a_2 should not be taken as exact but only as representative ranges of pore sizes, and these may form a more continuous distribution.

Table 1. Effect of Annealing on Pore Radii for a Typical Cellulose Acetate RO Membrane (from Chan[14])

radius of unshrunk membrane, $(R_b)_u \times 10^{10}$, m	radius of shrunk membranes, $(R_b)_s \times 10^{10}$, m	
	67 °C[a]	77 °C[a]
70.9	58.3	55.5
69.9	56.9	50.5
68.9	49.9	46.5
67.9	47.7	43.5
66.9	44.9	40.3
65.9	42.9	34.9
64.9	40.2	24.3
63.9	36.0	8.4
62.9	25.4	8.4
61.9	9.2	8.4
60.9	9.2	8.4
59.9	9.2	8.4
58.9	9.2	8.4
57.9	9.2	8.4
50.9	9.2	8.4
40.9	9.2	8.4
30.9	9.2	8.4
20.9	9.2	8.4
10.9	9.2	8.4
9.9	9.2	8.4

[a] Shrinkage temperature.

Finally, it is worthwhile to compare the results obtained in this study to those described by Chan.[14] His work involved the calculation of pore sizes for cellulose acetate RO membranes in an attempt to explain the changes occurring during the process of annealing a membrane. These calculations were based on experimental measurements of the rejection of certain test solutes by the membranes, using the "surface pressure–pore flow" model developed by Sourirajan.[15]

Chan determined the existence of two different distributions of pore sizes, one with average radius of 7–10 Å and the other with the average radius of 35–60 Å (pores > 100 Å in size are also present, but these are predominantly in the base layer of the membrane) in a typical RO membrane. He also described the effect of annealing an as-cast membrane on pore sizes and the pore size distribution. He concluded that there is only a moderate reduction in pore size during annealing for large (>60 Å pore radius) as well as for very small (<10 Å pore radius) pores. However, for pores in the intermediate region (10–60 Å pore radii) there is a drastic reduction in pore radius during annealing which shifts the radii of these "intermediate" pores toward the smaller of the two pore size distributions mentioned above (i.e., 7–10 Å). Table 1 shows the results of Chan for a typical RO membrane subjected to shrinkage (annealing). It can be seen that for a pore with relatively large radius, say 69 Å the reduction in pore radius is relatively small after annealing (final radius ~50 Å). However for a pore of radius ~ 60 Å, the decrease in pore size after annealing is dramatic (final pore radius ~ 10 Å).

The SANS results obtained in this work for *dry* RO membranes agree rather well with the calculations of Chan. As discussed earlier, the scattering data shows the presence of at least two different pore size distributions below 100 Å. In the present work the unannealed membrane contains no pores in the intermediate region (30–60 Å). The broadening of the pore size distribution after annealing, as evidenced by the shape of the scattering curve, is in good agreement with the changes in pore radii predicted in Table 1. It was mentioned earlier that the annealed membrane appears to contain a larger proportion of very small pores, and this observation is also in good accord with Chan's results, which indicate that the number of the very small pores increases with annealing (due to the shrinkage of the intermediate sized pores).

It must be noted that in the above discussion the data for the dry membrane were considered whereas Chan's calculations were performed for wet membranes. As discussed earlier, the differences between the unannealed and annealed membranes could not be observed in the D_2O swollen state presumably as a result of swelling effects. Thus it is highly likely that the differences between the two membranes *are present* in the swollen state but are *not detected* by the scattering technique.

Conclusions

Based on SANS experiments performed on cellulose acetate RO and UF membranes, the following conclusions can be drawn.

(1) The pore surface in UF membranes is smooth and nonfractal in nature.

(2) The estimates of pore sizes obtained for dry, D_2O swollen and CD_3OD swollen UF membranes agree well with pore sizes determined by electron microscopy. The difference in pore sizes between D_2O and CD_3OD swollen membranes can be related to the swelling abilities of the two solvents. A similar effect was observed in the case of cellulose acetate active layer membranes.

(3) Scattering from a dry unannealed RO membrane showed the presence of a fourth power law region at intermediate **Q**, implying an absence of pores in a certain size range in the membrane, and hence the existence of a rather sharply defined pore size distribution. The annealed membrane contained a much broader distribution of pore sizes. The observed differences between the unannealed and annealed membranes are in good agreement with the calculations of Chan.

(4) The intrinsic differences between the unannealed and annealed membranes are not evident in the case of the D_2O swollen membranes. This is most likely a result of swelling of the pores by the D_2O, which results in an overall broadening of the pore size distribution *as perceived* by small-angle scattering.

Acknowledgment. This research was supported in part by Grant CBT-8800649 from the National Science Foundation and in part by the Donors of the Petroleum Research Fund administered by the American Chemical Society. We wish to thank Dr. Takeshi Matsuura, National Research Council of Canada, for initiating us in the area of membrane preparation and for various valuable discussions. Work at Oak Ridge National Laboratory was supported by the U.S. Department of Energy, under contract DE-AC05-840R-21400 with Martin Marietta Energy Systems Inc. SANS data at NIST were taken on the 30 m instrument supported by the National Science Foundation under agreement No. DMR-9122444. Identification of certain equipment or products does not imply recommendation by the National Institute of Standards and Technology. We thank Dr. Boualem Hammouda for his assistance in performing the experiments at NIST.

References and Notes

(1) Kulkarni, S.; Krause, S.; Wignall, G. D.; Hammouda, B. *Macromolecules*, preceding paper in this issue.
(2) Kesting, R. E. *J. Appl. Polym. Sci.* **1990**, *41*, 2739.
(3) Manjikian, S.; Loeb, S.; McCutchan, J. W. *Proceedings of the 1st International Symposium on Water Desalination*, U.S. Dept. Interior; Office of Saline Water, Washington, D.C., 1965; Vol. 2, p 159.
(4) Loeb, S.; Sourirajan, S. *Adv. Chem. Ser.* **1962**, *38*, 117.

(5) Kunst, B.; Floreani, B. *Kolloid. Z. Z. Polym.* **1973**, *231*, 600.
(6) Lui, A.; Talbot, F. D. F.; Sourirajan, S.; Fouda, A.; Matsuura, T. *Sep. Sci. Tech.* **1988**, *23*, 1839.
(7) Moritani, M.; Inoue, T.; Motegi, M.; Kawai, H. *Macromolecules* **1970**, *3*, 433.
(8) Provencher, S. W. *J. Chem. Phys.* **1976**, *64*, 2722.
(9) Provencher, S. W. *Biophys. J.* **1976**, *16*, 27.
(10) Bale, H. D.; Schmidt, P. W. *Phys. Rev. Lett.* **1984**, *53*, 596.
(11) Schmidt, P. W. In *Characterization of Porous Solids*; Unger, K. K., Ed.; Elsevier Science Publishers B.V.: Amsterdam, 1988; pp 35–48.
(12) Porod, G. In *Small Angle X-Ray Scattering*; Glatter, O., Kratky, O., Eds.; Academic Press: New York, 1982; pp 29–32, 46–48.
(13) Statton, W. O. *J. Polym. Sci.* **1956**, *22*, 385.
(14) Chan, K.; Tinghul, L.; Matsuura, T.; Sourirajan, S. *Ind. Eng. Chem. Prod. Res. Dev.* **1984**, *23*, 124.
(15) Matsuura, T.; Sourirajan, S. *Ind. Eng. Chem. Process Des. Dev.* **1981**, *20*, 273.